Remote Sensing of Environment 280 (2022) 113145

Contents lists available at ScienceDirect

Remote Sensing of Environment

journal homepage: www.elsevier.com/locate/rse

Mowing detection using Sentinel-1 and Sentinel-2 time series for large scale grassland monitoring

Mathilde De Vroey [a,*], Laura de Vendictis [b], Massimo Zavagli [b], Sophie Bontemps [a], Diane Heymans [a], Julien Radoux [a], Benjamin Koetz [c], Pierre Defourny [a]

[a] Earth and Life Institute, Université catholique de Louvain, 2 Croix du Sud bte L7.05.16, 1348 Louvain-la-Neuve, Belgium
[b] Product Development and Innovative Services, e-GEOS, Via Tiburtina 965, 00156, Rome, Italy
[c] ESA-ESRIN, European Space Agency, Via Galileo Galilei, Casella Postale 64, 00044 Frascati, Rome, Italy

ARTICLE INFO

Edited by Jing M. Chen

Keywords:
Grasslands
Sen4CAP
Sentinel-1
Sentinel-2
Mowing detection

ABSTRACT

Managed grasslands cover about one third of the European utilized agricultural area. Appropriate grassland management is key for balancing trade-offs between provisioning and regulating ecosystem services. The timing and frequency of mowing events are major factors of grassland management. Recent studies have shown the feasibility of detecting mowing events using remote sensing time series from optical and radar satellites. In this study, we present a new method combining the regular observations of Sentinel-1 (S1) and the better accuracy of Sentinel-2 (S2) grassland mowing detection algorithms. This multi-source approach for grassland monitoring was assessed over large areas and in various contexts. The method was first validated in six European countries, based on Planet image interpretation. Its performances and sensitivity were then thoroughly assessed in an independent study area using a more precise and complete reference dataset based on an intensive field campaign. Results showed the robustness of the method across all study areas and different types of grasslands. The method reached a F1-score of 79% for detecting mowing events on hay meadows. Furthermore, the detection of mowing events along the growing season allows to classify mowing practices with an overall accuracy of 69%. This is promising for differentiating grasslands in terms of management intensity. The method could therefore be used for large-scale grassland monitoring to support agri-environmental schemes in Europe.

1. Introduction

Grasslands play an essential role in global food security, as they provide nearly half of the feed requirements of global livestock used for meat and milk production (Herrero et al., 2013; O'Mara, 2012). In Europe, managed grasslands cover about one third of the utilized agricultural area (UAA) and are a major part of the mixed pastoral and agricultural system. In addition to food production, grasslands contribute to regulating services such as carbon sequestration and water storage (Bengtsson et al., 2019; Chang et al., 2021) and they embed a rich biodiversity (O'Mara, 2012; Pärtel et al., 2005; Zeller et al., 2017). The ecological state and condition of European permanent grasslands, i.e. managed grasslands that have not been included in crop rotations for at least five years, is, however, threatened by agricultural intensification and conversion to annual crops (O'Mara, 2012; Silva et al., 2008). Maintaining permanent grasslands is therefore one of the main concerns of the European Common Agriculture Policy (CAP). Appropriate and spatially optimized management practices integrating knowledge of ecological processes are key for creating synergies and balancing trade-offs among the food production on one hand and regulating ecosystem services and biodiversity of grasslands on the other (Bengtsson et al., 2019; Chang et al., 2021; Pärtel et al., 2005; Savage et al., 2021). In this context, it is of great interest to be able to map and monitor grassland management practices at a large scale and with sufficient spatial resolution.

The intensity of mowing practices, i.e. the timing and frequency, is a major aspect of grassland management, along with grazing and fertilisation intensity. Studies showed that the timing and frequency of mowing events are positively correlated to forage yield and quality (Čop et al., 2009; Savage et al., 2021), while more extensive mowing practices maximize regulating ecosystem services and biodiversity (Kleijn et al., 2009; Pärtel et al., 2005; Savage et al., 2021; Uematsu et al., 2010; Van Vooren et al., 2018). Several studies have also highlighted the impact of different mowing practices on bird and butterfly species abundance, and

* Corresponding author.
E-mail address: mathilde.devroey@uclouvain.be (M. De Vroey).

https://doi.org/10.1016/j.rse.2022.113145
Received 17 January 2022; Received in revised form 28 April 2022; Accepted 21 June 2022

on plant diversity (Gerling et al., 2019; Humbert et al., 2012; Johansen et al., 2019; Morris and Rispin, 1987; Shahan et al., 2017; Tälle et al., 2018). Information on mowing events is therefore crucial for grassland management mapping and monitoring. It can furthermore be useful for habitat modelling.

Precise data on grassland mowing dates and frequency is, however, rarely available at a large scale, and monitoring mowing events through traditional field surveys is extremely time consuming. In this context, remote sensing can be a great asset. The increasing spatial resolution and revisit frequency of available satellite time series – especially with the recent Copernicus Sentinel missions – presents a considerable potential for large-scale grassland monitoring (Ali et al., 2016; Reinermann et al., 2020).

1.1. Optical remote sensing of grasslands

Optical remote sensing is largely and successfully used in agricultural mapping and monitoring (Ali et al., 2016; Reinermann et al., 2020). Indeed, the visible and near-infrared (IR) reflectance is strongly related to green biomass. Temporal profiles extracted from image time series allow to classify crop types (Belgiu and Csillik, 2018; Defourny et al., 2019) and monitor agricultural practices (Ottosen et al., 2019). In the case of grassland management monitoring, most studies use Normalized Difference Vegetation Index (NDVI) and Leaf Area Index (LAI) time series to differentiate between their types and intensities (Franke et al., 2012; Asam et al., 2015; Gómez Giménez et al., 2017; Hardy et al., 2021; Stumpf et al., 2020).

A number of studies have shown the potential of detecting mowing events through decreases in NDVI, as this vegetation index derived from red and near infra-red (NIR) bands is correlated with green biomass (Estel et al., 2018; Griffiths et al., 2020; Kolecka et al., 2018). Although they did not validate their results with ground truth data, Estel et al. (2018) discriminated the main grassland management patterns in Europe using MODIS NDVI mowing detection and livestock statistics. Using a validation dataset derived from visual interpretation of image time series, Kolecka et al. (2018) showed that 77% of mowing events were detected with Sentinel-2 (S2) NDVI. They stressed that the main challenge for grassland mowing detection is obtaining dense cloud-free time series. While large gaps due to persistent cloud cover can prevent the detection of mowing events, unmasked cloudy observations, causing an NDVI drop, could result in false detections. Kolecka et al. (2018) significantly improved their results by using an optimized blue-band based cloud masking algorithm. Griffiths et al. (2020) built 10-day composites from the harmonized Landsat S2 (HLS) dataset to reduce gaps due to cloud cover. More recently, Schwieder et al. (2022) showed that the impact of clear image availability on mowing detection by S2 and Landsat-8 is limited when at least 16 cloud-free observations are available during the season, while the temporal distribution of cloud-free observations remains critical.

1.2. SAR and grassland mapping

Ensuring regular and frequent observations can be a challenge using optical sensors, especially in regions with frequent cloud cover (Kolecka et al., 2018; Sano et al., 2007). SAR satellites carry active sensors, sending electromagnetic microwaves to the Earth's surface and measuring the backscattered signal amplitude and phase. Since active sensors are independent of sunlight and their microwaves are able to pass through cloud covers, SAR satellites provide regular observations through day and night. The backscattering intensity depends on sensor parameters (wavelength, polarization and incidence angle) and ground parameters (geometry, orientation and dielectric constant of soil and objects on the surface). A given signal interacts with objects and surface roughness with sizes larger or equal to its wavelength. C-band radars, such as Sentinel-1 (S1), have a wavelength of about 5 cm. They penetrate vegetation covers and interact with structural elements (leaves, branches), causing volume scattering. On bare soil or short vegetation, the backscattering intensity is influenced mostly by surface scattering.

Interferometric SAR (InSAR) measures the phase difference between two radar observations of the same area, taken from slightly different look angles. The interferometric coherence, which is a cross-correlation coefficient of two consecutive SAR observations, was initially computed to estimate phase noise for interferogram quality assessment. It has, however, also been exploited directly to estimate the temporal stability of ground targets. InSAR coherence has thereby been used for various applications including land cover mapping (Jacob et al., 2020; Strozzi et al., 2000), crop monitoring (Blaes et al., 1999; Shang et al., 2020) and soil moisture estimation (Barrett et al., 2009; De Zan et al., 2013; Rabus et al., 2010; Ulaby et al., 1979).

The potential of SAR data for detecting mowing events in grasslands has been shown in several studies. Although some studies accurately detect mowing events based on backscattering coefficient time series (Curnel, 2015; Schuster et al., 2011; Taravat et al., 2019), more promising results were obtained using interferometric coherence time series (De Vroey et al., 2021; Voormansik et al., 2020; Tamm et al., 2016).

On tall vegetation, the signal is dominated by volume scattering. Due to gradual growth of vegetation and random movements of tall grass in the wind, the distribution of scatterers changes between two acquisitions, causing temporal decorrelation of the signal and hence lower coherence values (Blaes et al., 1999; Monti-Guarnieri et al., 2020; Morishita and Hanssen, 2014; Voormansik et al., 2020). InSAR coherence is therefore relatively low on grasslands during their growing phase. After a mowing event, as the grass is cut short, the soil surface scattering, which is more stable over time, dominates the signal (Blaes et al., 1999). The coherence is therefore higher. Typical coherence profiles, showing lower values during the growing phase and high values after the mowing event, have been observed on aggregated time series of about 1000 mown grasslands (Voormansik et al., 2020; Tamm et al., 2016). Most mowing events can be detected in various permanent grasslands, based on jumps in smoothed S1 coherence time series (De Vroey et al., 2021). One of the main challenges in SAR is the speckle, an inherent variance caused by constructive and destructive interference between randomly distributed scatterers within a pixel (Lee et al., 1994). Even homogeneous surfaces such as intensively managed herbaceous covers thereby appear heterogeneous, which makes it challenging to work at sub-parcel level.

Moreover, InSAR coherence can be impacted by other factors than the biomass, such as soil moisture and vegetation water content (Ulaby et al., 1979; Barrett et al., 2009; Rabus et al., 2010; De Zan et al., 2013), which could hinder mowing detection as well.

1.3. Scope and objectives

The various studies discussed here show promising results suggesting the feasibility of automated grassland mowing detection through remote sensing. One of the keys for developing an accurate and robust mowing detection method is the quality and completeness of the reference data. Most of the above-mentioned studies, however, lack representative and precise reference data for validation and results can therefore rarely be generalized. In addition, the extent of the study area is often limited to one (or a few) region(s) with similar landscapes and agricultural practices. Moreover, many studies focus on exclusively mown – and often intensive – hay meadows. Information on types of grassland management is, however, rarely available. It should be noted that when applying optical or SAR based mowing detection methods on pastures and mixed practices (with both mowing and grazing activities), grazing was shown to be a confounding factor causing false mowing detections (De Vroey et al., 2021; Griffiths et al., 2020).

In this study, we present a new method combining the completeness of the S1 time series and the higher accuracy of S2 in a multi-source grassland mowing detection algorithm. The method was developed as a module of an open source toolbox, in the frame of the ESA-funded project Sentinels for Common Agricultural Policy (Sen4CAP), to facilitate the compliance assessment to several CAP subsidy schemes or support measures. The development and calibration of the method are not discussed extensively in this paper.

The objective of this paper is to introduce the operational Sen4CAP grassland mowing detection method, to validate its performances and to assess the potential of this multi-source approach for grassland monitoring over large areas. The method was first validated in the context of the Sen4CAP project in the six countries where it was developed. This validation was based on high-resolution image interpretation to rapidly build a large reference dataset. The method performances were then thoroughly assessed in an independent study area, using a more precise and complete dataset collected during an intensive field campaign. In addition, the grassland mowing detection by S1 was deeper investigated, more specifically regarding the impact of soil moisture on InSAR coherence and on the subsequent mowing detections, based on hourly precipitation data.

2. Method

The mowing detection method of Sen4CAP was developed, calibrated and refined in six pilot countries with varying climates and agricultural practices, namely Spain (ES), Czech Republic (CZ), Italy (IT), Lithuania (LT), the Netherlands (NL) and Romania (RO). The method consists of two independent object-based change detection algorithms based on S1 and S2 time series. Recent studies were considered as guidelines for feature and algorithm selection. S2 mowing detection was tested with normalized difference vegetation index (NDVI), leaf area index (LAI) and fraction of absorbed photosynthetically active radiation time series (fAPAR). S1 mowing detection was tested with backscattering and coherence in both VV and VH polarization. The available mowing date information in the pilot countries respective land parcel identification system (LPIS) data sets (i.e. a vector dataset based on legal declarations by farmers in each EU country, including parcel boundaries and crop types) were used as reference for the development, comparison and calibration of the detection algorithms. The resulting optimal combination of S1 and S2 features was S2 NDVI and S1 VH coherence time series.

In this paper, we describe and validate the operational grassland mowing detection method, available in the Sen4CAP toolbox v3.0 (Bontemps et al., 2022).

2.1. Satellite image processing

From S1, all Interferometric Wideswath (IW) L1C (Single Look Complex) images of the season, from S1 A and B satellites, in VH polarization, from both ascending and descending passes intersecting the regions of interest, are downloaded. The SNAP S1-toolbox (ESA, 2022, v6.0) is used to process the images. Each image is coregistered with all intersecting images acquired six days before. The interferometric coherence is computed between consecutive S1 A and B images from the same polarization and pass, in order to have a 6-day baseline instead of 12 (Tamm et al., 2016). The averaging window size is set to 5×20 pixels (in azimuth $\times$ range) for the calculation of the coherence. The processing chain further includes debursting, multilooking and terrain correction. The final resampled and ground projected images have a spatial resolution of 20 m $\times$ 20 m.

From S2, all available top of atmosphere L1C images of the season, intersecting the regions of interest are downloaded. The atmospheric correction and cloud detection are performed using the MACCS ATCOR Joint Algorithm (MAJA). The multi-temporal cloud detection method implemented in MAJA allows to produce a more consistent and accurate cloud and shadow mask compared to the one obtained by the Sen2COR algorithm used by ESA (Hagolle et al., 2010; Baetens et al., 2019). The resulting L2A images and validity masks are then used to produce cloud masked surface reflectance time series. Only images with less than 90% cloud cover are used. The NDVI is computed using the standard equation applied to S2's red (band 4) and narrow NIR (band 8a) bands.

The obtained features are then averaged per parcel to build S1 coherence time series and S2 NDVI time series. A ‘no-touch’ pixel sampling approach was applied, taking into account only pixels that are completely inside the parcel boundaries. This allows to limit border effects, while guaranteeing a sufficient number of pixels per parcel to mitigate the speckle of the SAR imagery.

2.2. Mowing detection algorithms

The grassland mowing detection method is object-based and applied independently on each parcel. Two separate change detection algorithms are applied for S1 and S2 time series. Results are merged into a single output for each parcel combining detections based on a reliability indicator.

The interferometric coherence is expected to increase after a mowing event because of the shorter vegetation, as explained in Section 1.2. The S1 algorithm therefore aims at detecting significant increases in coherence time series. Due to the growth of the vegetation, the coherence is expected to gradually decrease prior to a mowing event (Monti-Guarnieri et al., 2020; Morishita and Hanssen, 2014; Zalite et al., 2016). Therefore, each value $coh(t)$, extracted at time t, is compared to the value $coh\_fit(t - 1)$, predicted at time t - 1 by linear fit of the six previous values $[coh(t - 6), \ldots, coh(t - 1)]$. This allows to consider a potential slope in the coherence profile and detect sudden increases, compared to the previous signal trend. The detection is based on a Constant False Alarm Rate (CFAR) criterion (Eq. (1)).

$$coh(t). > coh\_fit(t-1) + k\sigma \tag{1}$$

The CFAR adaptive threshold ($k\sigma$) takes into account the standard deviation (σ) of the residual fitting errors, which are assumed to follow a Gaussian distribution in absence of a mowing event. The parameter k is fixed for a given probability of false alarm (PFA).

As for the S2-based algorithm, it aims at detecting significant decreases in the NDVI time series, while taking into account the irregular observation frequency due to cloud cover. Each observation $NDVI_{S2}(t)$, at time t, is compared to the last available cloud-free observation $NDVI_{S2}(t_{cf})$. The difference between $NDVI_{S2}(t)$ and $NDVI_{S2}(t_{cf})$ needs to be larger than a given threshold (Eq. (2)).

$$NDVI_{S2}(t). < NDVI_{S2}(t_{cf}) - th_{NDVI} \tag{2}$$

where th_{NDVI} is the fixed detection threshold.

In order to guarantee a minimum temporal precision despite the large gaps that can occur due to cloud cover, a maximum detection interval Δt_{max} is fixed. If an event is detected in the interval $[t_{cf},t]$ the actual mowing is expected to have occurred no more than Δt_{max} days before the low NDVI value at time t. If the time t - t_{cf} exceeds Δt_{max}, the detection interval in the output is then defined as $[t - \Delta t_{max}, t]$ instead. Table 1 shows the values of the detection thresholds and temporal parameters that were defined for the six pilot countries of the Sen4CAP project.

Fig. 1 illustrates the detection of mowing events based on S2 NDVI and S1 VH coherence separately, on a grassland parcel in the Netherlands.

Table 1
Parameters for the S1 and S2 mowing detection algorithm and their calibrated values for the Northern (NL, LT, CZ) and Southern (IT, ES, RO) pilot countries of the Sen4CAP demonstration.

Parameter	Symbol	North	South
Probability of False Alarm (S1)	PFA	3.0×10^{-7}	
NDVI absolute decreasing threshold (S2)	th_{NDVI}	0.12	0.15
Minimum time between two detections	Δt_{min}	28 days	
Maximum detection interval (S2)	Δt_{max}	60 days	

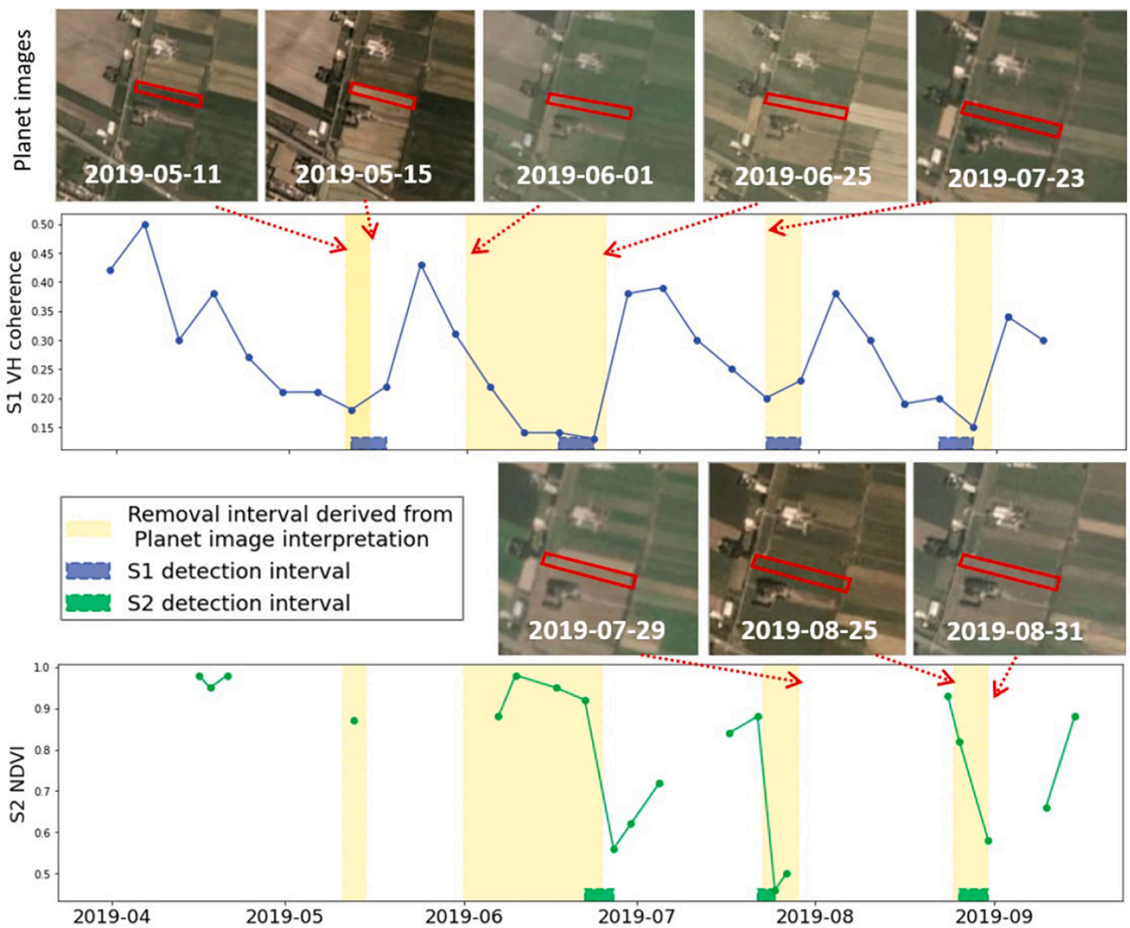

Fig. 1. Detection of mowing events on a grassland parcel in the Netherlands, based on S1 VH coherence and S2 NDVI and illustration of the validation from Planet image interpretation.

The confidence levels of S1 and S2 detections are estimated through a normalization function (Eq. (3)).

$$f(x; min, max) = max - (max - min) \times e^{-x} \tag{3}$$

Where x is the difference $coh(t) - coh\_fit(t-1)$ and $NDVI_{S2}(t_{cf}) - NDVI_{S2}(t) - th_{NDVI}$ for S1 and S2 respectively. The limits [min,max] are set to fit the confidence levels between separate range intervals ([0,0.5] for S1 and [0.5,1] for S2).

The confidence levels of overlapping S1 and S2 detections are then trivially merged. The four most confident detections, with a minimum interval Δt_{min} between $t_{start}(1)$ and $t_{end}(2)$ of consecutive detections, are retained. For each retained detection of each parcel, the time interval ($[t_{start}, t_{end}]$), the detection source (S1, S2 or S1 + S2) and the confidence level are provided as output.

2.3. Study areas and reference data

This paper presents the validation of the grassland mowing products obtained in the six pilot countries (ES, CZ, IT, LT, NL, RO) where the method was calibrated and a second independent validation based on ground truth data collected in Belgium.

2.3.1. Planet image interpretation

The validation of the mowing detection method in the six pilot countries was based on Planet image interpretation to obtain dates of biomass removal on a large set of grassland parcels.

For each country, a sample of about 100 to 200 parcels was randomly selected from the national LPIS datasets to be visually interpreted. The random selection was stratified in order to be statistically representative of national grassland parcels distribution in terms of management (e.g. pastures and meadows, permanent and temporary) and vegetation type (e.g. Alfalfa, clover, presence of orchids) with a minimum of five parcels per class. An exception to this rule was made in Castilla y Leon (ES), because the most abundant class (82%) was 'grassland pastures', which are mostly managed by grazing and not mowing. The fraction of mown grassland parcels in the Spanish sample was increased to 40% in order to include enough mowing events for validation. The selected samples, forming a total set of 803 grassland parcels across the six countries, are described in Fig. 2 and shown in Fig. 3.

The reference mowing dates were then obtained through visual interpretation of daily true-colour Planet images (average resolution: 3.5 m). For each parcel, the biomass removal intervals were identified, corresponding to the time interval between the last available cloud-free Planet image on which the grass seems to be tall (start date) and the first available cloud-free Planet image on which the grass seems to be short (end date) (Figs. 1 and 4 (a)). It is important to note that no clear distinction could be made between biomass removal by mechanical mowing or by intensive grazing.

Due to cloud cover, the length of the removal intervals varies, with a minimum of one day. A temporal buffer of three days was applied to the removal intervals to build the truth intervals for validation in order to compensate for the uncertainties inherent to the image interpretation. A longer buffer was applied after the removal intervals to take into account potential delayed detections due to grass left on the field to dry (Fig. 4 (a)).

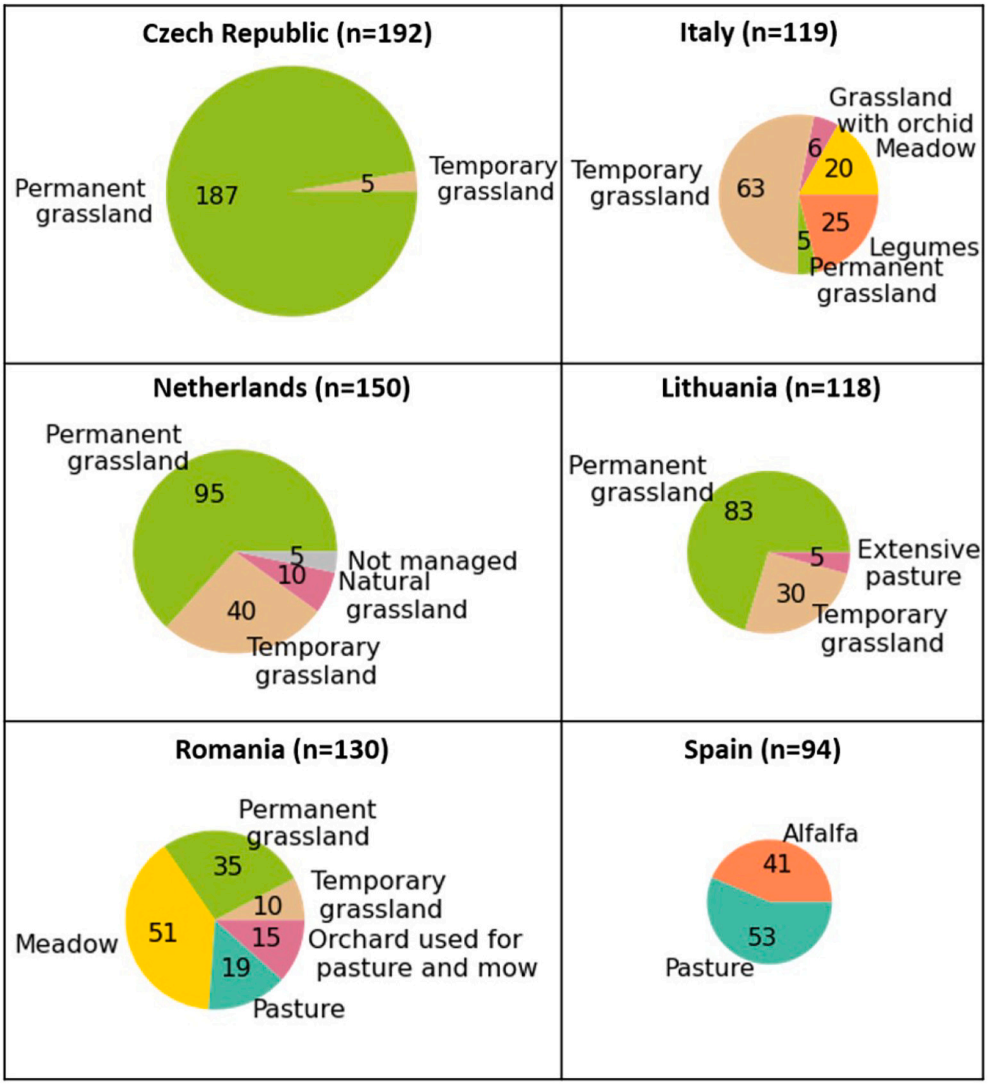

Fig. 2. Distribution of parcels per grassland type selected for validation in each pilot country.

2.3.2. *Independent field campaign*

An intensive field campaign was carried out in Wallonia, the Southern region of Belgium, to collect more precise and complete reference data for a fully independent performance assessment and to support a sensitivity analysis of the Sen4CAP mowing detection method.

The most common grasslands in Wallonia are permanent pastures and parcels managed by a relatively intensive combination of mowing and grazing. Extensive hay meadows which are strictly mown with no grazing activity, have become scarcer over the past decades (DEMNA, 2010). In most common grasslands, exploitation activities (grazing or mowing) start from mid-April. In grasslands of high biological interest, supported by the EU CAP, mowing is only allowed after the 16*th* of June, for flowering purposes, and before the 31*th* of October.

The field campaign was conducted from the 9*th* of April to the 19*th* of July 2019. During this period, we monitored 426 permanent grassland parcels (Fig. 5), including pastures, mixed practices and extensive hay meadows. Each parcel was monitored 11 times through a windshield survey. We made the hypothesis that the distance to the road did not affect the performance of the mowing detection by remote sensing. Visits were made with intervals of 6, 12 or 18 days with the highest frequency in May and June, when the first cuts are expected to occur and the regrowth would be relatively fast. On each visit, the management status of each grassland parcel was registered ('growing', 'recently cut', 'being cut', 'grazed'). This resulted in a time series of field observations for each parcel. Three types of intervals were defined based on subsequent field observations:

- Mowing intervals, corresponding to the time between the last observation marked as 'growing' (start date) and a 'recently cut'/ 'being cut' observation (end date) (Fig. 4 (b)) ;
- Grazing intervals, corresponding to a 'grazed' observation (end date), preceded by any other observation (start date) (Fig. 4 (c)) ;
- No activity intervals, corresponding to any observation (start date) followed by an observation marked as 'growing' (end date) (Fig. 4 (d)).

This survey resulted in a total of 4260 observation intervals (10 intervals for each of the 426 parcels) including 261 mowing intervals.

2.4. *Validation*

The performances of the mowing detection method were evaluated based on the different reference datasets and using three quality metrics, namely the *detection rate*, the *precision* and the the F1-score (Eqs. (4), (5) and (6)).

$$detection\ \ rate = \frac{TP}{(TP + FN)} \tag{4}$$

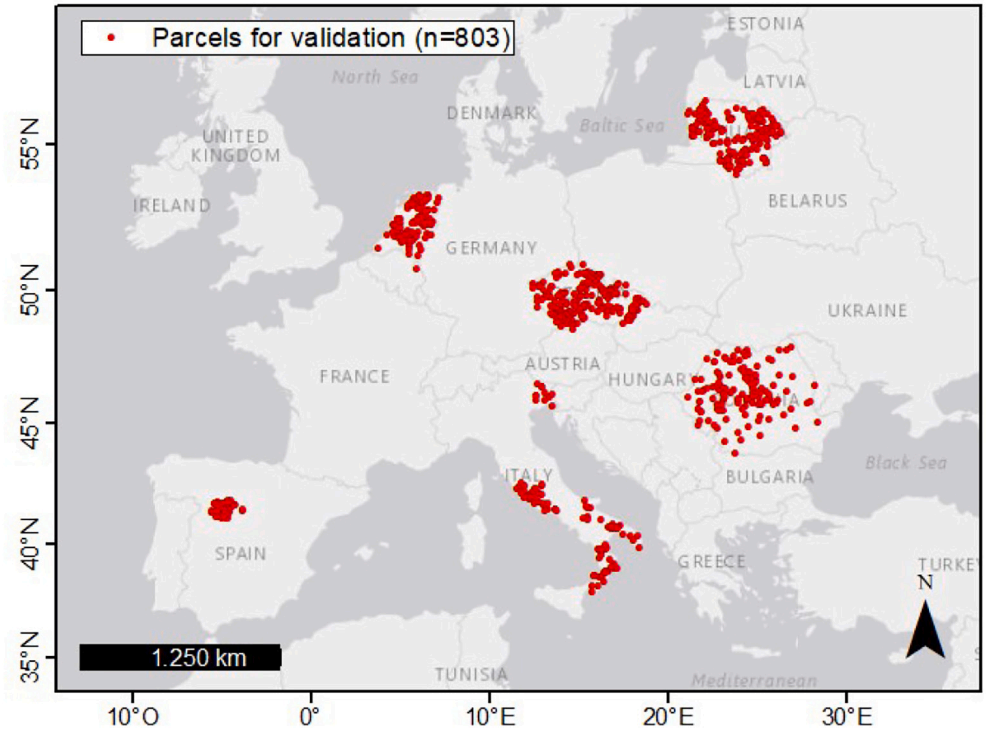

Fig. 3. Overview of the geographical distribution of parcels selected in the six Sen4CAP pilot countries to validate the grassland mowing detection method with Planet image interpretation.

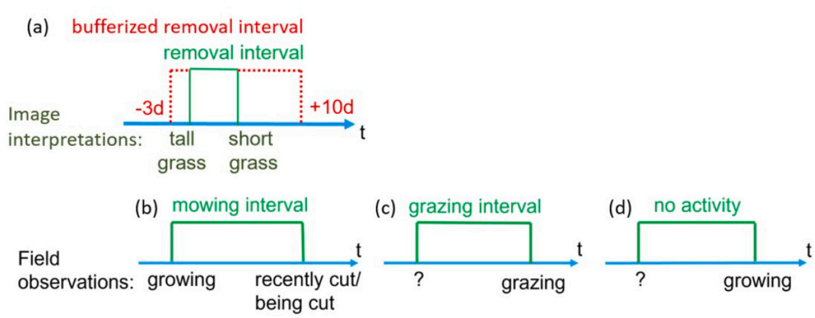

Fig. 4. Schematic representation of the different truth intervals defined by Planet image interpretation (a) and from the observations made during the field campaign on 426 grassland parcels in Wallonia (c-d).

$$precision = \frac{TP}{(TP + FP)} \tag{5}$$

$$F1_{score} = 2 \times \frac{precision \times detection\ rate}{precision + detection\ rate} \tag{6}$$

where TP, FP and FN are respectively the count of true positives, false positives and false negatives. These values are computed by crossing the reference datasets with detections at the temporal interval level. Each mowing detection is expressed as a temporal interval (t_{start} - t_{end}), in which the mowing probably occurred (i.e. detection interval). The reference data are also expressed in temporal intervals (i.e. truth intervals) (Sections 2.3.1 and 2.3.2).

When a detection interval intersects a truth interval, it is considered as a true positive (TP). If no truth interval overlaps a detection, it is a false positive (FP) and if no detection overlaps a truth interval, it is counted as false negative (FN). The remaining intervals are true negatives (TN).

Based on the TP, TN, FP and FN, the overall accuracy can be computed as well. It has to be noted that, given the relative rarity of mowing events, the overall accuracy is dominated by the numerous TN and therefore yields an overoptimistic summary of the performance of mowing detection.

2.5. Topsoil moisture as a potential confounding factor

In addition to the Sen4CAP mowing detection method validation, the impact of topsoil moisture on InSAR coherence was assessed as a potential confounding factor for the S1 mowing detection algorithm. This was done by estimating topsoil moisture at each S1 acquisition date and performing statistical hypothesis and separability tests on coherence values obtained in different topsoil moisture classes.

The antecedent precipitation index (API) (Linsley et al., 1949) was used as proxy for topsoil moisture. The API is a weighted summation of daily precipitation amounts. Hourly precipitation measurements were obtained from 11 weather stations of the Pameseb network of the Walloon Agronomic Research Center (CRA—W). The location of the 11 stations is shown in Fig. 5. Based on these measurements, the API at a

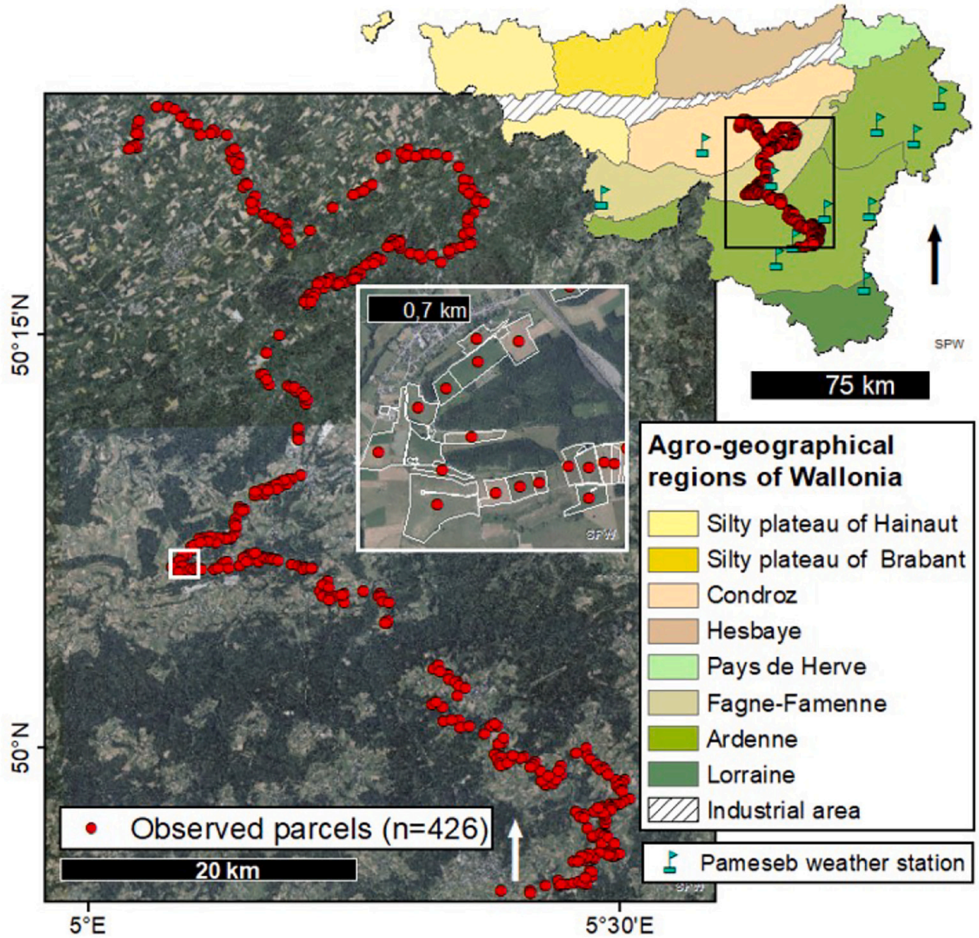

Fig. 5. Extent of the study area in Wallonia with (i) the location of the grassland parcels monitored during the field campaign and (ii) the 11 Pameseb weather stations from which hourly precipitation data were obtained.

time t was computed as follows (Eq. (7)).

$$API_t = r \times API_{t-\Delta t} + P_{\Delta t} \tag{7}$$

where r is a recession coefficient representing the rates of drainage and evapotranspiration processes. The commonly used value $r = 0.84$ was applied (Zhao et al., 2019). $P_{\Delta t}$ is the cumulative precipitation over the time Δt, fixed here at one day.

Coherence time series were extracted for all permanent grassland parcels of the LPIS in a 5 km radius around each station, resulting in a total of 6966 parcels. The soil in the parcels around a station at time t was considered as 'wet' if API_t was in the upper quartile (0.75) of the station's values and as 'dry' if it was in the lower quartile (0.25). Each

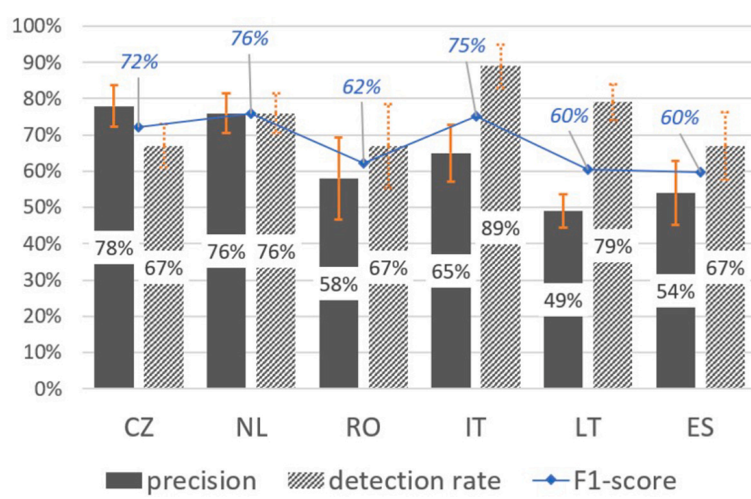

Fig. 6. Precision, detection rate and F1-score of the Sen4CAP mowing detection method estimated based on a visually interpreted reference dataset in six countries: Spain (ES), Czech Republic (CZ), Italy (IT), Lithuania (LT), the Netherlands (NL) and Romania (RO). The confidence interval of each metric is indicated in orange.

six-day interferometric pair of dates at each station could thereby be characterized as 'wet-wet', 'dry-dry', 'dry-wet' or 'other' if it did not correspond to any of these three classes. The coherence values of each class were then compared through statistical hypothesis tests and separability measures. The tests were performed on S1 data from the descending and ascending pass separately, as the different acquisition times - respectively around 6 a.m. and 6 p.m. - could alter the impact of topsoil moisture on the signal (e.g. dew in the morning).

3. Results

3.1. Large extent validation based on Planet imagery

The main results of the validation in the six pilot countries of the Sen4CAP project are shown on Fig. 6. These results show statistically significant differences of precision and detection rates among the countries. The differences could be related to the type of grassland parcels used for validation (cfr. Fig. 2) as well as to the climate and landscape characteristics of each country.

The best F1-score (76%) is achieved in the Netherlands, where the *precision* and the *detection rates* are equal. Italy and Lithuania have the largest *detection rate* (89% and 79%), but are penalized by a lower *precision*.

The highest *detection rates* occur in regions with a large amount of temporary grasslands in the validation datasets. This can be explained by the larger biomass removal in the usually more productive temporary grasslands, but we did not have enough data to rigorously test this hypothesis in the scope of this study.

The highest *precision* is obtained in Czech Republic and in the Netherlands. These two Northern countries also show the most balanced and confident performances. On the other hand, the prevalence of grazing practices could explain the lower precision obtained in Spain and Lithuania (54% and 49% respectively).

In Spain and Romania, the drying of grass in the summer also needs to be considered as a confounding factor for Planet image interpretation as well as for the mowing detection algorithms, especially if grasslands are managed through mixed grazing and mowing practices. In Italy, the drought, although present, seems to have less impact on the mowing detection performances. This can be explained by the prevalence of temporary grasslands, which are generally mown (not grazed) earlier in the season and therefore less affected by drought. The Southern countries (RO, ES, IT) are all characterized by a larger confidence interval, compared to the Northern countries (CZ, NL, LT). An additional analysis on the parcel size revealed no significant effect on the mowing detection performances across the pilot countries (Bontemps et al., 2021).

3.2. Field based validation and performance assessment

In the 426 permanent grasslands observed during the field campaign across Wallonia, the Sen4CAP mowing detection method reached an overall accuracy of 97% and a F1-score of 58%. This independent validation showed a high *detection rate* of 83%, but the *precision* was relatively low, with only 44% of the detection intervals being true positives (i.e. actual mowing events).

A more detailed analysis of the false positives reveals potential sources of error (Table 2). First of all, almost half of the false positives overlapped a grazing interval in the reference dataset. In the remaining cases, no activity was observed at the time of the detection. When discarding all parcels where grazing was observed, and taking exclusively mown parcels into account, the *precision* increases to 73%, as a large part of the false positives are removed. The *detection rate* is also slightly higher (85%). This results in a F1-score of 79% and an OA of 99%.

In terms of detection sources, 54% of the false positives were based on S1 only, the remaining being almost equally distributed between S2 and S1 + S2 (24% and 22% respectively).

Finally, a majority (64%) of false positives occurred after the 20*th* of June.

Table 2
Detailed analysis of false positives, highlighting potential sources of error for the Sen4CAP mowing detection using S1 and S2. Number (n) and fraction (%) of false positives per (i) observed activity at the time of detection, (ii) detection source of the detection and (iii) detection before or after June 20.

FALSE POSITIVES ($n = 268$, commission error = 56%)		
Categories	n	%
Field observation		
no activity	139	52%
grazing	129	48%
Detection source		
S1	145	54%
S2	64	24%
S1 + S2	59	22%
Timing of the detection		
early event ($\leq$ June 20)	91	34%
late event (> June 20)	177	66%

Further analysis of the mowing detection sources shows the complementarity of S1 and S2. Fig. 7 (a) shows the *precision* and *detection rate* obtained using S2 and S1 algorithms alone, compared to the results achieved by the combined algorithms. The *precision* is highest when using S2 alone (59%), compared to 45% with S1 only and 44% with both. The *detection rate,* however, is largely improved, up to 83% with the combined detections, compared to 69% for each individual algorithm. Fig. 7 (b) shows the distribution of true and false positives per detection source when applying the combined algorithms. 80% of detections by S1 alone are false positives. The number of detections by S2 alone is relatively low, with a small majority of false positives. The most certain detections are those confirmed by both satellites (72% TP for S1 + S2).

The confidence level computed for each detection provides valuable information about their certainty. Fig. 8 shows the *precision* and the number of detections for different confidence level intervals. Most detections have a confidence level between 0.4 and 0.6 and between 0.8 and 0.9. Under a confidence level of 0.4 less than 10% of the detections are true positives. Above a confidence level of 0.2, the *precision* is strongly correlated to the confidence level ($R^2 = 0.94$).

Finally, mowing detection performances were also analysed per parcel to assess the ability of the method to identify different types of mowing practice observed during the field campaign in terms of frequency and precocity of mowing events (ME) ('no ME', '1 early ME', '1 late ME' and '2 ME'). Fig. 9 (a) shows the results considering all detections. As expected based on previous analyses, most false positives occur in parcels that were not mown during the study period, resulting in a low fraction (32%) of correctly identified 'no ME' parcels. From the parcels with 1 early ME and 1 late ME, respectively 58% and 76% are identified correctly. Most errors in these classes are due to an additional false positive. In the '2 ME' class, 76% of the parcels are identified correctly and almost all errors are due to the omission of the first (early) ME.

The same evaluation was performed after filtering out detections with confidence levels below 0.5 in order to reduce the number of false positives (Fig. 9 (b)). This significantly improves the results on 'no ME' parcels, as more than twice as many are then identified correctly (69%). Although more ME are omitted, performances are also slightly improved for parcels with 1 ME (from 58% to 60% for early ME and from 78% to 83% for late ME). Performances on parcels with 2 ME, however, are much lower (24%) as the first ME is often omitted. Given that most omissions seem to occur for early ME, which are crucial for grassland use intensity assessment, the minimum confidence level could be adapted to the time of the season.

A third test was performed considering early detections with a minimum confidence level of 0.4 and late detections with a minimum of 0.5 (Fig. 9 (c)). This enhances the results on parcels with no ME (67%), while maintaining a reasonable *detection rate* of early events (74%) in

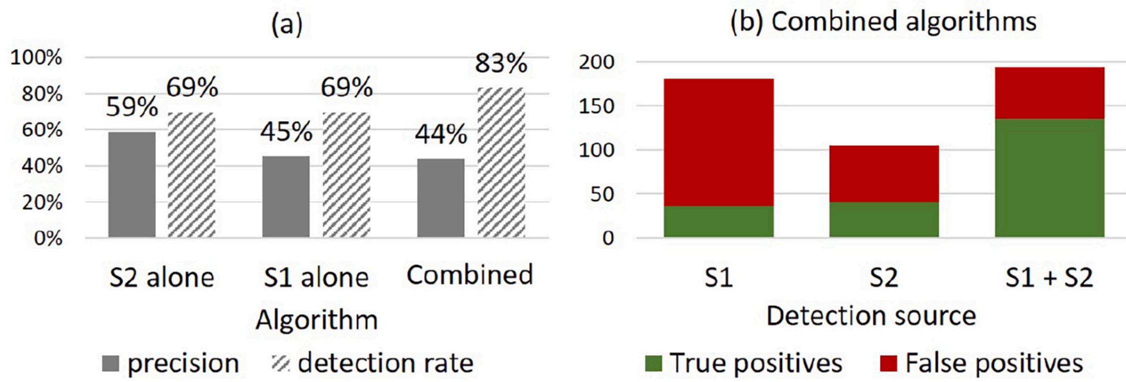

Fig. 7. (a) Mowing detection performances (*precision* and *detection rate*) of algorithms based on S1 and S2 time series alone compared to the merged approach. (b) Distribution of true and false positives per detection source (S1, S2 or S1 + S2) when applying the merged approach.

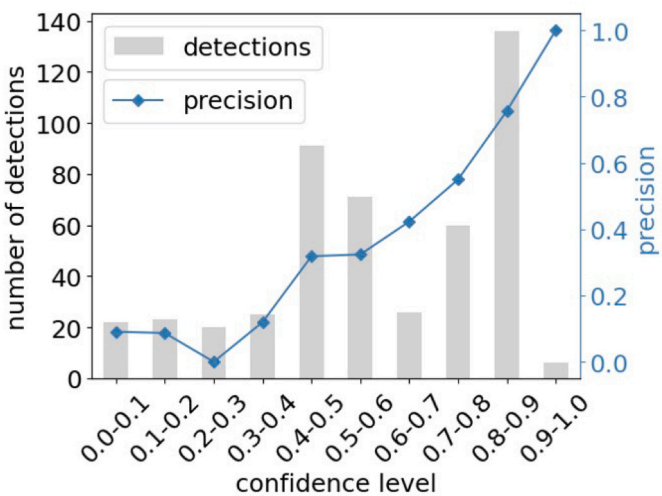

Fig. 8. *Precision* and number of detections per given confidence level.

parcels with '2 ME'. With this adaptive minimum confidence level, 69% of all parcels are identified correctly in terms of mowing practice, compared to 51% when taking all detections into account.

3.3. Algorithm sensitivity

In order to assess the sensitivity of the algorithm, it was tested with different parameter configurations in the Walloon study area. The parameter values defined in Table 1 for Northern countries were used as a baseline. We compared the *detection rates* and *precisions* obtained when increasing or decreasing these parameter values.

The impact of different PFA and th_{NDVI} values on the *detection rate* and *precision* are shown in Fig. 10 (a) and (b). When increasing the PFA for S1 mowing detection from 3×10^{-7} to 3×10^{-6} or 3×10^{-5} the loss in *precision* is greater than the gain in *detection rate*, lowering the overall performance. When decreasing the PFA to 3×10^{-8}, the *precision* is slightly enhanced, while the *detection rate* is a bit lower. When changing the th_{NDVI} for S2 detection either to 0.10, 0.14 or 0.20, the loss is systematically more important than the gain in *precision* or *detection rate*. Overall, the changes in performances are relatively small in the range of tested threshold values, showing a small sensitivity to the algorithm parameter values.

The analysis of the temporal parameters Δt_{max} and Δt_{min} is shown in Fig. 11. With a maximum detection interval of 60 days, most detection intervals don't exceed 24 days (Fig. 11 (a)), although the region is relatively cloudy, meaning a Δt_{max} of 60 days may be excessively cautious. When decreasing Δt_{max} down to 18 days and thereby reaching a higher temporal precision, there is no loss in *detection rate* (Fig. 11 (b)). At a Δt_{max} of 12 days, however, some detections become false positives, since the true mowing event was observed earlier. This results in a lower *detection rate* and *precision*. The minimum time Δt_{min} of 28 days between

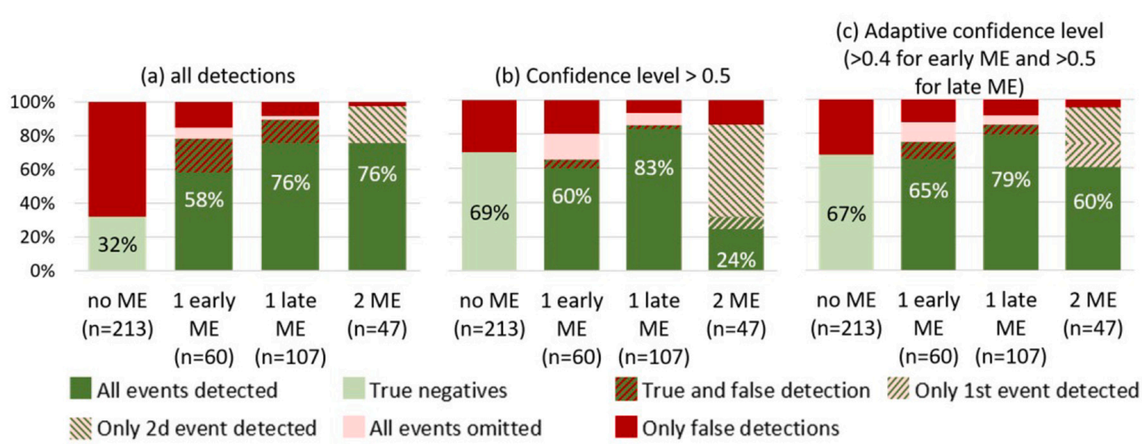

Fig. 9. Mowing detection evaluation per type of observed mowing practice, considering (a) all detections, (b) detections associated with a confidence level above 0.5 and (c) using an adaptive minimum confidence level for early and late detections. For each option, the fraction of correctly estimated parcels is given, along with the types of errors that occur (false positives, omissions or both).

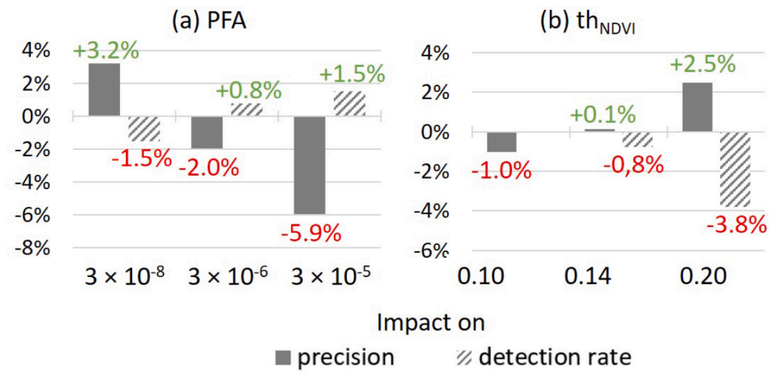

Fig. 10. Sensitivity of the mowing detection algorithm calibration. Impact of two threshold parameters: (a) probability of false alarm (PFA) for S1 detection and (b) NDVI decreasing absolute threshold (th_{NDVI}) on *detection rate* and *precision*, compared to the calibrated parameter values.

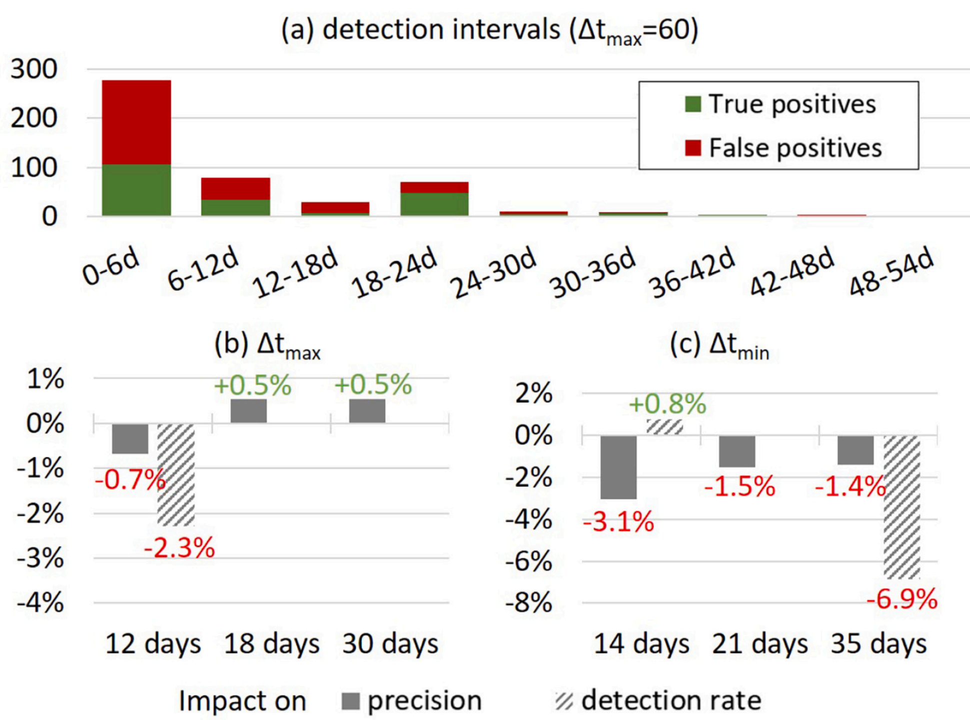

Fig. 11. (a) Distribution of true and false positives per detection interval category Δt. Impact of (b) maximum detection interval (Δt_{max}) and of (c) minimum interval (Δt_{min}) between consecutive detections on *detection rate* and *precision*, compared to the calibrated parameter values.

two consecutive detections, on the other hand, seems to be an adequate choice (Fig. 11 (c)). Reducing Δt_{min} (to 21 or 14 days) or increasing it (to 35 days) has an overall negative effect on the detection accuracy.

These different results confirm that the standard set of parameter values (Table 1) for the Northern European countries seems most appropriate.

3.4. Impact of soil moisture on interferometric coherence

The distributions of S1 coherence values of grassland parcels in different topsoil moisture classes ('wet-wet', 'dry-dry', 'dry-wet' and 'others') were compared in order to assess the impact of soil moisture on coherence (Fig. 12). Although the distributions of the four classes have significant overlaps, coherence values are slightly higher in average for the 'dry-dry' class than for the 'wet-wet' or 'dry-wet' classes. Coherence is also slightly higher for the 'wet-wet' class than for the 'dry-wet' one.

The coherence distributions of each class were compared through a statistical hypothesis test. The resulting *p*-values are given in Table 3, along with the histogram intersections and the absolute differences between the averages (bias). The p-values are extremely low because of the large sample sizes ($n_{min} \approx 11000$) used to compute the averages, which are indeed different from one class to another. The histogram intersections are however high, showing very limited separability between the coherence values of the different topsoil moisture classes. The smallest intersection (71%) is between 'dry-dry' and 'dry-wet'. These two classes also show the largest bias between their respective average coherence values, with coherences higher by 0.06 for the 'dry-dry' class. As it is more diverse, the 'others' class shows the least difference and separability with the three extreme classes. Overall, these results show that slightly higher coherence values can be expected on grasslands during consecutive dry periods. Important precipitations, resulting in 'dry-wet' and 'wet-wet' classes, cause slightly lower coherence on average, due to signal decorrelation.

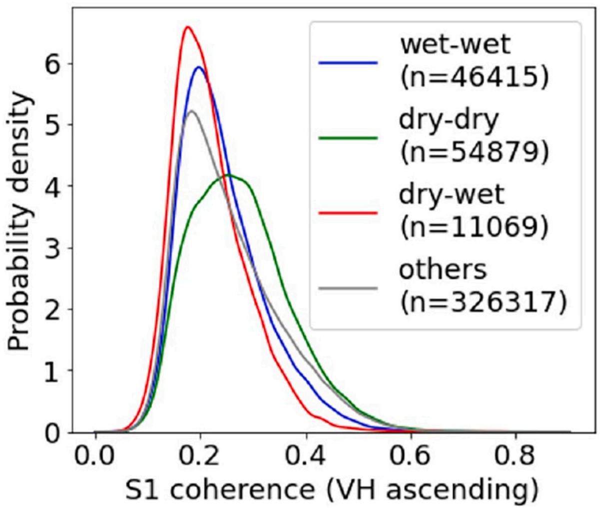

Fig. 12. Distribution of S1 coherence (VH ascending) values for different topsoil moisture classes in grassland parcels.

Table 3
Comparison of S1 coherence (VH ascending) values distributions in different soil moisture classes. In each cell, the table shows the statistical *t*-test *p*-values (top), the histogram intersection (centre) and the bias (bottom) between classes.

Soil moisture classes	dry-dry	dry-wet	others
wet-wet	$< 10^{-5}$ 82% −0.03	$< 10^{-5}$ 81% 0.02	$< 10^{-5}$ 91% −0.01
dry-dry		$< 10^{-5}$ 71% −0.06	$< 10^{-5}$ 86% 0.02
dry-wet			$< 10^{-5}$ 84% −0.03

4. Discussion

4.1. Complementarity of S1 and S2

Optical vegetation index time series have been used previously for detecting mowing events, providing overall satisfying results (Griffiths et al., 2020; Kolecka et al., 2018; Schwieder et al., 2022). These methods, however, rely on the availability of cloud-free images before and, more importantly, after an event. Depending on the region of interest, this condition cannot always be met. During the growing season in Belgium for example, there are only 4 to 6 days per month with less than 20% cloud cover and 6 to 11 days per month with more than 80% cloud cover (Meteoblue, 2021). Such a persistent cover, which is frequent in Northern European countries, strongly reduces the actual observation frequency of S2. Griffiths et al. (2020) used the HLS dataset (from 2016, before Sentinel-2B was launched) and compositing to build a regular NDVI time series and obtained promising results. Their biggest drawback was however the significant amount of omitted mowing events. Schwieder et al. (2022) developed a similar method, based on HLS (with the complete Sentinel-2 constellation) and detecting anomalies, compared to an idealized grassland phenology curve. Their results on hay meadows (F1-score 58-67%) are comparable with those obtained in this study, on meadows and pastures, when using S2 alone. Their detection method however included more conservative detection rules and thresholds to avoid false detections (e.g. due to unmasked clouds), gaining in *precision*, but omitting more events.

SAR imagery represents a great asset for mowing detection in cloudy areas, as microwaves are transmitted through clouds. Our results are consistent with previous studies, showing that mowing events can be detected through jumps in InSAR coherence time series (De Vroey et al., 2021; Voormansik et al., 2020; Tamm et al., 2016). Detections by S1 are, however, less precise than by S2. This was confirmed by our analysis of the detection sources in the Walloon study area. The SAR signal can be impacted by many factors outside the reduction of biomass, such as soil and vegetation moisture. On the descending pass, images are acquired in the early morning (around 6 a.m.). Since both passes are used to build S1 time series for the detection, the effect of morning dew on the SAR signal could be a possible explanation to the lower performances. The signal decorrelation due to increased soil moisture, thus preventing coherence to rise after a mowing event, is a potential cause for omissions (Section 3.4). Applying a systematic bias correction would, however, require a cautious investigation because of the variability of the soil moisture impact. Overall, the complex interaction of SAR signal with object and surfaces, and the inherent speckle of SAR imagery, make it more challenging to interpret.

Despite the challenges inherent to SAR based methods, the combination of S1 and S2 detection algorithms in this multi-source method significantly increased the *detection rate*. Some of the events that were omitted by S2 due to cloud cover could be detected by S1. Conversely, events that were omitted by S1 due to change in soil moisture or other confounding factors, could be detected by S2 when a clear image was available shortly after the event.

Moreover, the estimated confidence levels, based on the normalization of the amplitude of the signal change and used to merge the S1 and S2 detections, were shown to be well correlated to the *precision* of the detection. They are consequently a good indicator of the probability of occurrence of a mowing event and can be used to screen out detections according to the final use, in order to be more or less conservative.

The complementarity of optical and radar imagery for mowing detection was also recently confirmed by Lobert et al. (2021) with a deep learning approach. In their study, they compared different combinations of S1, S2 and Landsat-8 features in a convolutional neural network (CNN). All combinations of optical and SAR features outperformed exclusive uses of either optical or SAR features. NDVI and coherence was their fifth best performing combination, with a detection rate (recall) of 85% and a precision of 79%. From a fully independent validation, we obtained comparable results on hay meadows in Wallonia, using similar input features in a versatile and transparent rule-based change detection method.

Overall, recent studies on automated grassland mowing detection seem to show coherent results and conclusions. Multi-source mowing detection methods combining optical and SAR data should be further investigated and developed.

4.2. Reference data and validation

Although previous studies showed the feasibility of mowing detection through satellite remote sensing, they often lacked sufficient precise and complete reference data to calibrate and validate their methods (Reinermann et al., 2020). Information on mowing dates and practices is rarely readily available and collecting it in situ is extremely time consuming.

Image time series interpretation offers a cost effective and less time consuming alternative for grassland mowing detection validation, as a unique reference dataset or as a complement to smaller samples of reported or observed mowing events (Griffiths et al., 2020; Schwieder et al., 2022). In this study, the Planet image interpretation approach allowed to rapidly gather a large reference dataset ($n = 803$) to validate the mowing detections in six countries along the whole season (April to October 2019). However, the reliability of this reference dataset was limited for a number of reasons. First, persistent cloud coverage prevented the observation of some events in Northern countries. Secondly, the absence of the NIR band in the Planet Web Mapping Service available for the Sen4CAP partners limited the certainty of observations due to confusion with ploughing events and grassland droughts in the Southern countries. Finally, the varying radiometric and geometric precision of Planet images, depending on the satellites that acquire the data, increased the uncertainty of the interpretation.

Overall, there is a risk of non independence between the reference data and the classification results due to the similarity of criteria used by the machine and by the image interpreters. This non independence could introduce a bias in the estimation of accuracy indices (Radoux and Bogaert, 2020).

The second validation dataset acquired through an intensive field campaign is much more complete, more accurate, and fully independent of the classification rationale. This dataset allowed to estimate the *detection rate* and the *precision* of the mowing detection method with more certainty, to test its transferability and evaluate its potential for grassland use intensity assessment. While the results of the Planet-based validation reflect the ability of the method to detect grassland biomass removal, regardless if by mowing or intensive grazing, the field dataset of Wallonia allowed to validate the detection of actual mowing events (differentiating them from grazing). During the field-based validation, mowing detections overlapping grazing intervals were considered as false positives, which strongly reduced the computed *precision*. Half of the false positives were confirmed as intensive grazing events. Such detections would be considered as true positives in the Planet-based validation since there was no distinction between mowing and grazing in the reference dataset.

In addition to - and depending on - the source and quality of reference data, the performances of a mowing detection method can be evaluated at different levels. In this study, we used a conservative validation approach, which reflects the ability to exactly detect the occurrence and the timing of each mowing event and allows to compute explicit metrics such as the *precision*, *detection rate* and F1-score (Lobert et al., 2021; De Vroey et al., 2021; Schwieder et al., 2022). With such an approach, a delayed or untimely detection is counted as a false negative and a false positive. Therefore, we performed an additional analysis per parcel, to assess the ability of the method to identify different types of mowing practice in terms of frequency and precocity of ME. Another possible approach is to validate the frequency and the exact timing of mowing events separately (Griffiths et al., 2020; Schwieder et al., 2022). With this approach, a delayed (or untimely) detection is only considered as an error in terms of timing, since the mowing frequency is accurate. In general, a combination of different levels of performance evaluation provides the best and most complete estimation of a methods potential and limitations and allows to compare results between studies.

4.3. Diversity of practices

Given the diversity of climates, landscapes and grassland managements across Europe, it is challenging to develop a grassland mowing detection method that is adapted to all regions. Part of the dissimilarities in mowing detection performances between the pilot countries can indeed be explained by climate. While more mowing events are omitted in Northern regions due to cloud cover, drought can cause false detections and reduce the precision of the method in Southern regions.

The method accurately detects removal of grass biomass and works best on permanent grasslands managed as hay meadows. Most studies on grassland mowing detection focus on permanent hay meadows. However, from an operational point of view, we wanted to assess its performances on diverse grassland management types because precise land cover and land use information is not always available. The various types of grasslands in the pilot countries, i.e. more or less intensive, temporary or permanent, pastures or meadows, vegetation types, etc. can also explain part of the discrepancies in the results.

The performances of the mowing detection method in different grassland types could however not be assessed quantitatively, because of the limited available information and the lack of uniformity between the countries respective LPIS grassland categories. In many cases, the categories remain subject to interpretation in terms of management type and intensity. For example, in Romania a distinction is made between meadows and pastures, while some grasslands are classified more generally as permanent grasslands. In Italy and Spain, grasslands include leguminous crops. In Czech Republic, the Netherlands and Lithuania, a majority of parcels are classified as permanent grasslands, which could be either mown or grazed, more or less intensively.

The field dataset collected in Wallonia was restricted in terms of land cover to permanent grasslands dominated by gramineous plants, but included all types of agricultural land use, namely pastures, meadows and mixed practices. The regular field observations provided more precise information about the management of each parcel. This allowed to analyse the mowing detection performances with regards management types. In any case, the SEN4CAP algorithm performed as expected. On one hand, under the same conditions, late ME are better detected than early ME. Detection may be hindered because of faster regrowth of grass in the spring, making it more challenging to spot the smaller decrease in biomass. Detecting early mowing events is however crucial for grassland use intensity assessment. Increasing the *detection rate* to capture the early ME however implies to sacrifice some *precision*. On the other hand, grazing practices that engender a large biomass removal in a short period of time (e.g. intensive rotational grazing) are a major confounding factor. Without information about the location of hay meadows, increasing the *precision* in areas with intensive pasture therefore requires to sacrifice the *detection rate*.

Other practices can potentially prevent the accurate detection of mowing events by S1 and S2. For example, when cut grass is left on the parcel to dry during a few days after a mowing event, it can influence the signal and prevent an accurate change detection.

Finally, it must also be considered that the management practices might not be homogeneous at the parcel-level. Indeed, the full parcel, as declared in the LPIS, is not always mown at the same time (e.g. in the case of rotating intra-parcel management). In an object-based approach, partial mowing of parcels risk being omitted as both mown and unmown pixels contribute to the average parcel value, reducing the apparent change in the time series. Pixel-based mowing detection approaches using optical imagery have shown promising results (Griffiths et al., 2020; Kolecka 411 et al., 2018; Schwieder et al., 2022). Monitoring grasslands at the pixel level allows to account for intra-parcel variability in terms of practices, but on the other hand, it causes a salt and pepper effect that is avoided in an object-based approach. Moreover, while optical pixel-based mowing detection is feasible, the speckle effect inherent to SAR imagery would probably be a significant issue for SAR pixel-based mowing detection. Furthermore, the combination of S1 and S2 mowing detection at pixel level would be more complex and imply a resampling step. Another option would be to use S1 and S2 data fusion methods simulating optical images (Garioud et al., 2021; He and Yokoya, 2018) to work at the pixel level while compensating for cloud cover.

Overall, the multi-source mowing detection method presented here detects mowing events with a relatively high accuracy and allows to consistently differentiate various mowing practices and grassland use intensity trends across different agro-geographical regions. It can be adapted by changing the detection threshold parameters to optimize the balance between *detection rate* and *precision*, depending on the context and objective of its use. Furthermore, the final result can be filtered, based on the provided confidence level, as it is a good indicator for the reliability of the detections. The mowing detection method of Sen4CAP could thereby be used for large-scale grassland monitoring and even mapping ecological habitat quality.

5. Conclusion

This study showed the full potential and limitations of Sen4CAP's multi-source mowing detection method based on S1 and S2 time series. The exhaustive reference datasets allowed to show the consistency of the algorithm across seven European countries and various types of grasslands, while highlighting the importance of reference data quality. Thanks to the complementary use of S1 and S2, the method reached a *detection rate* of 85% and a *precision* of 73% (F1-score 79%) for detecting mowing events on hay meadows. Furthermore, the detection of mowing events along the growing season allows to classify mowing practices with an overall accuracy of 69% and should allow to differentiate grasslands in terms of management intensity.

Further efforts are still needed to improve the mowing detection accuracy and produce a more precise and thematically more complete grassland management map. Nevertheless this adaptive and transparent mowing detection method could be implemented in large-scale grassland monitoring. Combined with ecological modelling tools, it could be used to support agro-environmental schemes in Europe.

Author responsibilities

Mathilde De Vroey: Conceptualization, Validation, Formal analysis, Writing - Original Draft, Writing - Review & Editing; Laura de Vendictis: Conceptualization, Methodology, Validation, Formal analysis; Massimo Zavagli: Conceptualization, Methodology, Validation, Formal analysis; Sophie Bontemps: Conceptualization, Writing - Original Draft, Supervision; Diane Heymans: Conceptualization, Validation, Writing - Original Draft; Julien Radoux: Conceptualization, Validation, Writing - Original Draft, Supervision; Benjamin Koetz: Conceptualization, Supervision, Writing - Review & Editing; Pierre Defourny: Conceptualization, Writing - Original Draft, Supervision.

Declaration of Competing Interest

The authors declare that they have no known competing financial interests or personal relationships that could have appeared to influence the work reported in this paper.

Acknowledgements

The grassland mowing detection method was developed and validated as part of Sentinels for Common Agricultural Policy - Sen4CAP - which was set up and funded by ESA. The field campaign and subsequent analysis were supported by LifeWatch FWB in the context of the ESFRI and funded by Fédération Wallonie Bruxelles.

References

Ali, I., Cawkwell, F., Dwyer, E., Barrett, B., Green, S., 2016. Satellite remote sensing of grasslands: from observation to management. J. Plant Ecol. 9, 649–671.
Asam, S., Klein, D., Dech, S., 2015. Estimation of grassland use intensities based on high spatial resolution LAI time series. In: ISPRS - International Archives of the Photogrammetry, Remote Sensing and Spatial Information Sciences XL-7/W3, pp. 285–291.
Baetens, L., Desjardins, C., Hagolle, O., 2019. Validation of copernicus Sentinel-2 cloud masks obtained from Maja, Sen2Cor, and FMask processors using reference cloud masks generated with a supervised active learning procedure. Remote Sens. 11, 433.
Barrett, B.W., Dwyer, E., Whelan, P., 2009. Soil moisture retrieval from active spaceborne microwave observations: an evaluation of current techniques. Remote Sens. 1, 210–242.
Belgiu, M., Csillik, O., 2018. Sentinel-2 cropland mapping using pixel-based and object-based time-weighted dynamic time warping analysis. Remote Sens. Environ. 204, 509–523.
Bengtsson, J., Bullock, J., Egoh, B., Everson, C., Everson, T., O'Connor, T., O'Farrell, P., Smith, H., Lindborg, R., 2019. Grasslands—more important for ecosystem services than you might think. Ecosphere 10, e02582.
Blaes, X., Defourny, P., Derauw, D., Barbier, C., 1999. InSAR coherence for crop parameter monitoring. In: Proc. FRINGE, Citeseer, pp. 10–12.
Bontemps, S., de Vendictis, L., Malcorps, P., Sciarretta, C., Zavagli, M., 2021. Sen4CAP - Sentinels for Common Agriculture Policy - Validation Report.
Bontemps, S., Bajec, K., Cara, C., Defourny, P., de Vendictis, L., Heymans, D., Kucera, L., Malcorps, P., Milcinski, G., Nicola, L., Slacikova, J., Taymans, M., Tutunaru, F., Udroiu, C., 2022. Sen4cap - Sentinels for Common Agricultural Policy. http://esa-sen4cap.org/content/download-package-description.
Chang, J., Ciais, P., Gasser, T., Smith, P., Herrero, M., Havlík, P., Obersteiner, M., Guenet, B., Goll, D.S., Li, W., et al., 2021. Climate warming from managed grasslands cancels the cooling effect of carbon sinks in sparsely grazed and natural grasslands. Nat. Commun. 12, 1–10.
Čop, J., Vidrih, M., Hacin, J., 2009. Influence of cutting regime and fertilizer application on the botanical composition, yield and nutritive value of herbage of wet grasslands in Central Europe. Grass Forage Sci. 64, 454–465.
Curnel, Y., 2015. Satellite Remote Sensing Priorities for Better Assimilation in Crop Growth Models: Winter Wheat LAI and Grassland Mowing Dates Case Studies. Ph.D. thesis. UCL-Université Catholique de Louvain.
De Vroey, M., Radoux, J., Defourny, P., 2021. Grassland mowing detection using Sentinel-1 time series: potential and limitations. Remote Sens. 13, 348.
De Zan, F., Parizzi, A., Prats-Iraola, P., López-Dekker, P., 2013. A SAR interferometric model for soil moisture. IEEE Trans. Geosci. Remote Sens. 52, 418–425.
Defourny, P., Bontemps, S., Bellemans, N., Cara, C., Dedieu, G., Guzzonato, E., Hagolle, O., Inglada, J., Nicola, L., Rabaute, T., et al., 2019. Near real-time agriculture monitoring at national scale at parcel resolution: performance assessment of the Sen2-Agri automated system in various cropping systems around the world. Remote Sens. Environ. 221, 551–568.
DEMNA, 2010. Les prairies et les pelouses (E) - biotopes - la Biodiversité en Wallonie. http://biodiversite.wallonie.be/fr/prairies-et-pelouses-e.html?IDC=815. Accessed: 01.12.2020.
ESA, 2022. v6.0. Sentinel application platform (snap). http://step.esa.int.
Estel, S., Mader, S., Levers, C., Verburg, P.H., Baumann, M., Kuemmerle, T., 2018. Combining satellite data and agricultural statistics to map grassland management intensity in Europe. Environ. Res. Lett. 13, 074020.
Franke, J., Keuck, V., Siegert, F., 2012. Assessment of grassland use intensity by remote sensing to support conservation schemes. J. Nat. Conserv. 20, 125–134.
Garioud, A., Valero, S., Giordano, S., Mallet, C., 2021. Recurrent-based regression of sentinel time series for continuous vegetation monitoring. Remote Sens. Environ. 263, 112419.
Gerling, C., Sturm, A., Wätzold, F., 2019. Ecological-economic modelling to compare the impact of organic and conventional farming on endangered grassland bird and butterfly species. Agric. Syst. 173, 424–434.
Gómez Giménez, M., de Jong, R., Della Peruta, R., Keller, A., Schaepman, M.E., 2017. Determination of grassland use intensity based on multi-temporal remote sensing data and ecological indicators. Remote Sens. Environ. 198, 126–139.
Griffiths, P., Nendel, C., Pickert, J., Hostert, P., 2020. Towards national-scale characterization of grassland use intensity from integrated Sentinel-2 and Landsat time series. Remote Sens. Environ. 238, 111124.
Hagolle, O., Huc, M., Pascual, D.V., Dedieu, G., 2010. A multi-temporal method for cloud detection, applied to FORMOSAT-2, VENμS, Landsat and Sentinel-2 images. Remote Sens. Environ. 114, 1747–1755.
Hardy, T., Kooistra, L., Domingues Franceschini, M., Richter, S., Vonk, E., van den Eertwegh, G., van Deijl, D., 2021. Sen2Grass: a cloud-based solution to generate field-specific grassland information derived from Sentinel-2 imagery. AgriEngineering 3, 118–137.
He, W., Yokoya, N., 2018. Multi-temporal Sentinel-1 and-2 data fusion for optical image simulation. ISPRS Int. J. Geo Inf. 7, 389.
Herrero, M., Havlík, P., Valin, H., Notenbaert, A., Rufino, M.C., Thornton, P.K., Blümmel, M., Weiss, F., Grace, D., Obersteiner, M., 2013. Biomass use, production, feed efficiencies, and greenhouse gas emissions from global livestock systems. Proc. Natl. Acad. Sci. 110, 20888–20893.
Humbert, J.Y., Pellet, J., Buri, P., Arlettaz, R., 2012. Does delaying the first mowing date benefit biodiversity in meadowland? Environ. Evid. 1, 1–13.
Jacob, A.W., Vicente-Guijalba, F., Lopez-Martinez, C., Lopez-Sanchez, J.M., Litzinger, M., Kristen, H., Mestre-Quereda, A., Ziółkowski, D., Lavalle, M., Notarnicola, C., et al., 2020. Sentinel-1 InSAR coherence for land cover mapping: a comparison of multiple feature-based classifiers. IEEE J. Sel. Top. Appl. Earth Obs. Remote Sens. 13, 535–552.
Johansen, L., Westin, A., Wehn, S., Iuga, A., Ivascu, C.M., Kallioniemi, E., Lennartsson, T., 2019. Traditional semi-natural grassland management with heterogeneous mowing times enhances flower resources for pollinators in agricultural landscapes. Glob. Ecol. Conserv. 18, e00619.
Kleijn, D., Kohler, F., Báldi, A., Batáry, P., Concepción, E.D., Clough, Y., Díaz, M., Gabriel, D., Holzschuh, A., Knop, E., Kovács, A., Marshall, E.J.P., Tscharntke, T., Verhulst, J., 2009. On the relationship between farmland biodiversity and land-use intensity in Europe. Proc. R. Soc. B Biol. Sci. 276, 903–909.
Kolecka, N., Ginzler, C., Pazur, R., Price, B., Verburg, P.H., 2018. Regional scale mapping of grassland mowing frequency with Sentinel-2 time series. Remote Sens. 10, 1221.
Lee, J., Jurkevich, L., Dewaele, P., Wambacq, P., Oosterlinck, A., 1994. Speckle filtering of synthetic aperture radar images: a review. Remote Sens. Rev. 8.
Linsley, R.K., Kohler, M.A., Paulhus, J.L., 1949. Applied hydrology. In: Technical Report.
Lobert, F., Holtgrave, A.K., Schwieder, M., Pause, M., Vogt, J., Gocht, A., Erasmi, S., 2021. Mowing event detection in permanent grasslands: systematic evaluation of input features from Sentinel-1, Sentinel-2, and Landsat 8 time series. Remote Sens. Environ. 267, 112751.
Meteoblue, 2021. Simulated Historical Climate & Weather Data for Brussels. https://www.meteoblue.com/en/weather/historyclimate/climatemodelled. Accessed: 2021-05-21.
Monti-Guarnieri, A., Manzoni, M., Giudici, D., Recchia, A., Tebaldini, S., 2020. Vegetated target decorrelation in SAR and interferometry: models, simulation, and performance evaluation. Remote Sens. 12, 2545.
Morishita, Y., Hanssen, R.F., 2014. Temporal decorrelation in L-, C-, and X-band satellite radar interferometry for pasture on drained peat soils. IEEE Trans. Geosci. Remote Sens. 53, 1096–1104.
Morris, M., Rispin, W., 1987. Abundance and diversity of the coleopterous fauna of a calcareous grassland under different cutting regimes. J. Appl. Ecol. 451–465.

O'Mara, F.P., 2012. The role of grasslands in food security and climate change. Ann. Bot. 110, 1263–1270.
Ottosen, T.B., Lommen, S.T., Skjøth, C.A., 2019. Remote sensing of cropping practice in northern Italy using time-series from Sentinel-2. Comput. Electron. Agric. 157, 232–238.
Pärtel, M., Bruun, H.H., Sammul, M., 2005. Biodiversity in temperate European grasslands: origin and conservation. In: Grassland science in Europe. Grassland Science in Europe, pp. 1–14.
Rabus, B., Wehn, H., Nolan, M., 2010. The importance of soil moisture and soil structure for InSAR phase and backscatter, as determined by fdtd modeling. IEEE Trans. Geosci. Remote Sens. 48, 2421–2429.
Radoux, J., Bogaert, P., 2020. About the pitfall of erroneous validation data in the estimation of confusion matrices. Remote Sens. 12, 4128.
Reinermann, S., Asam, S., Kuenzer, C., 2020. Remote sensing of grassland production and management—a review. Remote Sens. 12, 1949.
Sano, E.E., Ferreira, L.G., Asner, G.P., Steinke, E.T., 2007. Spatial and temporal probabilities of obtaining cloud-free Landsat images over the brazilian tropical savanna. Int. J. Remote Sens. 28, 2739–2752.
Savage, J., Woodcock, B.A., Bullock, J.M., Nowakowski, M., Tallowin, J.R., Pywell, R.F., 2021. Management to support multiple ecosystem services from productive grasslands. Sustainability 13, 6263.
Schuster, C., Ali, I., Lohmann, P., Frick, A., Förster, M., Kleinschmit, B., 2011. Towards detecting swath events in TerraSAR-x time series to establish NATURA 2000 grassland habitat swath management as monitoring parameter. Remote Sens. 3, 1308–1322.
Schwieder, M., Wesemeyer, M., Frantz, D., Pfoch, K., Erasmi, S., Pickert, J., Nendel, C., Hostert, P., 2022. Mapping grassland mowing events across Germany based on combined sentinel-2 and landsat 8 time series. Remote Sens. Environ. 269, 112795.
Shahan, J.L., Goodwin, B.J., Rundquist, B.C., 2017. Grassland songbird occurrence on remnant prairie patches is primarily determined by landscape characteristics. Landsc. Ecol. 32, 971–988.
Shang, J., Liu, J., Poncos, V., Geng, X., Qian, B., Chen, Q., Dong, T., Macdonald, D., Martin, T., Kovacs, J., et al., 2020. Detection of crop seeding and harvest through analysis of time-series Sentinel-1 interferometric SAR data. Remote Sens. 12, 1551.
Silva, J.P., Toland, J., Jones, W., Eldridge, J., Thorpe, E., O'Hara, E., 2008. LIFE and Europe's Grasslands, Restoring a Forgotten Habitat. https://ec.europa.eu/environment/archives/life/publications/life-publications/lifefocus/documents/grassland.pdf.
Strozzi, T., Dammert, P.B., Wegmuller, U., Martinez, J.M., Askne, J.I., Beaudoin, A., Hallikainen, N., 2000. Landuse mapping with ERS SAR interferometry. IEEE Trans. Geosci. Remote Sens. 38, 766–775.
Stumpf, F., Schneider, M.K., Keller, A., Mayr, A., Rentschler, T., Meuli, R.G., Schaepman, M., Liebisch, F., 2020. Spatial monitoring of grassland management using multi-temporal satellite imagery. Ecol. Indic. 113, 106201.
Tälle, M., Deák, B., Poschlod, P., Valkó, O., Westerberg, L., Milberg, P., 2018. Similar effects of different mowing frequencies on the conservation value of semi-natural grasslands in Europe. Biodivers. Conserv. 27, 2451–2475.
Tamm, T., Zalite, K., Voormansik, K., Talgre, L., 2016. Relating Sentinel-1 interferometric coherence to mowing events on grasslands. Remote Sens. 8, 802.
Taravat, A., Wagner, M.P., Oppelt, N., 2019. Automatic grassland cutting status detection in the context of spatiotemporal Sentinel-1 imagery analysis and artificial neural networks. Remote Sens. 11, 711.
Uematsu, Y., Koga, T., Mitsuhashi, H., Ushimaru, A., 2010. Abandonment and intensified use of agricultural land decrease habitats of rare herbs in semi-natural grasslands. Agric. Ecosyst. Environ. 135, 304–309.
Ulaby, F.T., Bradley, G.A., Dobson, M.C., 1979. Microwave backscatter dependence on surface roughness, soil moisture, and soil texture: part ii-vegetation-covered soil. IEEE Trans. Geosci. Electron. 17, 33–40.
Van Vooren, L., Reubens, B., Broekx, S., Reheul, D., Verheyen, K., 2018. Assessing the impact of grassland management extensification in temperate areas on multiple ecosystem services and biodiversity. Agric. Ecosyst. Environ. 267, 201–212.
Voormansik, K., Zalite, K., Sünter, I., Tamm, T., Koppel, K., Verro, T., Brauns, A., Jakovels, D., Praks, J., 2020. Separability of mowing and ploughing events on short temporal baseline Sentinel-1 coherence time series. Remote Sens. 12, 3784.
Zalite, K., Antropov, O., Praks, J., Voormansik, K., Noorma, M., 2016. Monitoring of agricultural grasslands with time series of X-band repeat-pass interferometric SAR. IEEE J. Sel. Top. Appl. Earth Obs. Remote Sens. 9, 3687–3697.
Zeller, U., Starik, N., Göttert, T., 2017. Biodiversity, land use and ecosystem services—an organismic and comparative approach to different geographical regions. Glob. Ecol. Conserv. 10, 114–125.
Zhao, B., Dai, Q., Han, D., Dai, H., Mao, J., Zhuo, L., Rong, G., 2019. Estimation of soil moisture using modified antecedent precipitation index with application in landslide predictions. Landslides 16, 2381–2393.